Materials Advances

ROYAL SOCIETY OF CHEMISTRY

PAPER

View Article Online
View Journal | View Issue

Cite this: *Mater. Adv.*, 2023, 4, 4843

Synthesis and characterization of a high-performance bio-based Pebax membrane for gas separation applications

R. Surya Murali, *[ab] Amit Jha,[a] Aarti,[ab] Swapnil Divekar[ab] and Soumen Dasgupta[ab]

Bio-based polymers with at least a portion of the polymer derived from renewable raw materials have been the subject of research due to the increasing worldwide inclination towards sustainability. The synthesis of bio-based polymeric membranes is required to reduce dependency on fossil fuels. Pebax® Rnew® 30R51 (Pebax Rnew) is a type of bio-based polymer consisting of polyether segments and polyamide segments, wherein the polyamide segments are obtained from renewable sources. This study focuses on synthesizing and characterizing Pebax Rnew membranes for gas separation applications. Pebax Rnew was dissolved in a solvent mixture of 1-butanol and 1-propanol and cast on a Petri dish, followed by complete solvent evaporation. Free-standing dense membranes of 2 wt%, 4 wt%, 6 wt% and 8 wt% polymer solution concentration were synthesized. Pure CO_2, H_2, CH_4, N_2 and O_2 gas permeabilities were measured at ambient temperature and pressures varying from 2–10 bar, and the corresponding ideal selectivities were calculated. The synthesized membrane surface and cross-sectional morphologies were investigated by scanning electron microscopy. Thermogravimetric analysis, Fourier-transform infrared spectroscopy and X-ray diffraction studies were conducted to determine the thermal stability, intermolecular interactions and intersegment distance between the polymer chains. For a 6 wt% Pebax Rnew membrane, a high permeability of 205 Barrer was measured for CO_2, whereas the CH_4, O_2 H_2, and N_2 permeabilities were 9.6, 8.1, 2.9 and 18.6 Barrer, respectively. With increasing pressure, the selectivity was enhanced from 65 to 91, 20 to 26 and 9.7 to 13.5 for CO_2/N_2, CO_2/CH_4 and CO_2/H_2 gas systems, respectively. This work provides scope for developing bio-based membranes comparable with existing membranes for different gas separation applications to achieve process targets.

Received 10th July 2023,
Accepted 7th September 2023

DOI: 10.1039/d3ma00385j

rsc.li/materials-advances

1. Introduction

Membrane-based gas separation processes are an efficient technology to reduce carbon emissions and achieve carbon neutrality. Polymeric membranes are commercially widely used in industrial separation applications due to their low cost, ease of processing and mechanical properties. Over the decades, various membranes have performed well in separating CO_2 from N_2 in coal-fired power plants.[1,2] CO_2 separation from CH_4 is another primary industrial application of membranes in refineries to meet natural gas pipeline specifications and increase the calorific value of the stream.[3] Similarly, CO_2 and H_2S can be separated from biogas using membranes.[4] Membrane separation processes are an attractive alternative for separating H_2 and N_2 from an ammonia purge stream and CO_2 from H_2 in the water–gas shift reaction to produce enriched H_2.[5,6] Another interesting membrane application is CH_4 and N_2 separation from coal-bed methane gas. Membrane-based air separation plays a significant role in the chemical industry in producing enriched nitrogen and oxygen.[7]

The selection of a polymer material is crucial in developing a membrane for gas separation. One of the methods to overcome the trade-off challenge is to combine flexible polyether polymers with mechanically stable and rigid polymers such as polyamides.[8] A poly(ether block amide) copolymer is such type of material that consists of both linear chains of flexible polyether segments (PE) and hard polyamide segments (PA). Glassy polyamide segments contribute mechanical strength, whereas rubbery polyether segments provide high permeability owing to the higher polymer chain mobility of the ether functional groups.[9] Poly(ether block amide) thermoplastic elastomers is best known by the trademark Pebax. Different grades of Pebax copolymers are being synthesized by changing the composition of the amide and ether segments.

[a] *Separation Process Division, CSIR-Indian Institute of Petroleum, Dehradun, 248005, India. E-mail: surya.racha@iip.res.in*
[b] *Academy of Scientific and Innovation Research (AcSIR), Sector 19, Kamla Nehru Nagar, Ghaziabad 201002, Uttar Pradesh, India*

Table 1 Composition of different grades of Pebax copolymers studied for gas separation applications

Pebax grade	Rigid polyamide segment	Flexible polyether segment	Rigid polyamide segment wt%	Flexible polyether segment wt%	Ref.
1657	PA6[a]	PEO[d]	40	60	9
2533	PA12[b]	PTMO[e]	20	80	13
1074	PA12	PEO	45	55	14
3533	PA12	PTMO	25	75	15
4033	PA12	PTMO	43	57	16
5533	PA12	PTMO	70	30	11
4011	PA6	PEO	43	57	11
Rnew® 30R51	PA11[c]	PEO	20	80	17

[a] PA6:5 methyl units polyamide. [b] PA12:11 methyl units polyamide. [c] PA11:10 methyl units polyamide. [d] PEO: poly(ethylene oxide). [e] PTMO: polytetramethylene oxide.

Researchers have been developing and modifying different Pebax grades for various gas separation studies.[10–16] Table 1 illustrates the composition of Pebax grades that are majorly evaluated for gas separation applications. Pebax has been extensively studied for CO_2 separation application owing to its strong affinity among CO_2 gas molecules and polar carbonyl linkages present in the PE blocks.[8–10] Bondar *et al.*[11] evaluated the different grades of Pebax membranes for gas separation properties, materials such as Pebax 2533, 4033, 1074 and 4011. It was revealed that gas permeability increases with increasing the percentage of the PE blocks in the Pebax copolymers. Researchers have been extensively working on Pebax 1657 due to its higher CO_2 permeation properties.[9–12]

Currently, the majority of membranes used for separation applications are synthetic polymeric materials. These synthetic polymers are usually produced from fossil-based resources, which leads to anthropogenic emission of greenhouse gas that significantly contributes to climate change. Hence, it is essential to switch from a fossil-based materials economy to an ideally circular materials economy. Development of biobased polymers is an alternative to solve the environmental impact and dependency on fossil resources. This transition generates an opportunity to develop sustainable membrane materials for separation applications.[18]

Bio-based polymers are materials for which at least a portion of the polymer is formed from renewable raw materials.[19] Biopolymers or monomers are commonly obtained from plants, biogenic feed stocks and other non-fossil resources. A blend of renewable resource monomers and fossil-based monomers is also referred to as biobased polymer materials.[20] Based on the current progress in circular materials and green environmental regulations, biomaterials are renowned as impending and sustainable materials for switching with fossil-based synthetic polymers. Bio-based polymeric membrane materials have been used in microfiltration, ultrafiltration, reverse osmosis, gas separation and pervaporation applications.

Pebax® Rnew® 30R51 is a variety of biobased polymers made of flexible polyether segments derived from fossil fuel and rigid polyamide segments from renewable sources. Castor seeds obtained from castor plants are the base material for preparing renewable polyamide segments. These castor beans are initially crushed followed by pressing to extract the oil. The thus obtained castor oil is processed through several refining steps and finally transformed into amino-11 monomers. The synthesized monomers are further processed into polyamides (PA11). Pebax Rnew polymer is synthesized by the polycondensation of renewable polyamides (PA11) with an alcohol-terminated polyether.[21]

Martínez-Izquierdo *et al.* synthesized Pebax Rnew membranes for single and mixed gas permeation studies. Compared to other Pebax grades, 1657 and Rnew exhibited superior separation performance due to the presence of polyethylene oxide as the soft segments, which show more interaction with CO_2 gas molecules. A 3 wt% Pebax Rnew membrane exhibited a CO_2 permeability of 167 and 164 Barrer for single and mixed gas permeation, respectively, and corresponding CO_2/N_2 selectivities of 41 and 37 were calculated.[8] The higher solubility of CO_2 in the case of Pebax Rnew has increased research interest in focusing on membrane preparation parameters and their modification. The same group modified membranes by incorporating an ionic liquid (IL) [Bmim][BF_4] and metal–organic framework (MOF) to prepare thin film composite (TFC) membranes *via* spin coating on polysulfone supports. Compared with the Pebax Rnew TFC membrane, the IL loading improved the CO_2 permeance by 27% and CO_2/N_2 selectivity by 7%. Whereas, MOF incorporation increased CO_2 permeance by 51% and 65% for ZIF-8 and ZIF-94, respectively, although the CO_2/N_2 separation selectivity decreased by 7% to 25 in both cases.[17]

Polymer solution concentration plays a significant role in membrane formation and separation performance. The viscosity of a polymer solution increases with polymer concentration and reaches a critical concentration, where beyond critical concentration entanglement of the polymer chains is inevitable. Martínez-Izquierdo *et al.* studied the influence of casting solution concentration on the morphology and gas permeation properties of Pebax-1657 membranes. The polymer crystallinity, an important factor in the fabrication of organized structures, decreased with increasing polymer concentration from 1 wt% to 5 wt%. Membranes prepared from a 3 wt% Pebax-1657 solution were found to exhibit higher separation performance, irrespective of the operating temperature.[22] Similarly, Hasan *et al.* synthesized Pebax-3533 membranes by varying the concentration from 1 wt% to 6 wt% and evaluated them for CO_2 separation. Increasing the polymer concentration enhanced the performance from 1 wt% to 5 wt% and higher concentrations resulted in a decrease in membrane performance due to changes in polymer crystallinity.[23]

We believe that solution concentration effects could help in selecting a suitable polymer concentration for gas separation applications. It is essential to find a correlation among the casting conditions and membrane performance, including morphology, thermal and mechanical properties, long term stability, *etc.* To our knowledge, for Pebax Rnew membranes, the effect of polymer concentration on morphology, thermal and complete gas permeation properties has not been discussed previously in the literature. In this work, Pebax® Rnew® 30R51 (Pebax Rnew) membranes were synthesized and the permeability of pure CO_2, CH_4, H_2, N_2 and O_2 gases was evaluated. This study intended to assess the effect of polymer concentration on gas permeabilities.

Further, membrane performance was investigated by varying the feed gas pressure. The physical and chemical characteristics of the membranes were evaluated using scanning electron microscopy (SEM), Fourier-transform infrared (FTIR) spectroscopy, X-ray diffractometry (XRD) and thermogravimetric analysis (TGA) characterization.

2. Materials and methods

2.1. Materials

Arkema India Chemicals Private Limited, Mumbai, kindly provided Pebax® Rnew® 30R51 as pellets. Fig. 1 shows the chemical structure of the Pebax Rnew polymer, which contains 20% rigid polyamide and 80% flexible polyether segments. Castor oil extracted from castor plant seeds was used to produce the basic building blocks of the polyamide PA11 (https://pebaxpowered.arkema.com/en/bio-based-pebax/). Fig. 2 shows the steps involved in synthesizing the Pebax Rnew polymer, which consists of 45% bio content, according to ASTM D6866.[24]

Chemicals for membrane synthesis were used as received without any purification. ACS grade 1-butanol and 1-propanol were purchased from Alfa Aesar, India. CO_2, CH_4, H_2, O_2, and N_2 gas cylinders of >99.9% purity were supplied by Sigma Gases and Services, India.

2.2. Membrane preparation

The membranes were synthesized using solution casting and a controlled solvent evaporation method. Pebax Rnew membranes were cast from polymer solution containing 2 wt% to 8 wt% polymer in a 1:1 solvent mixture of 1-butanol and 1-propanol under constant stirring of around 400 rpm at a temperature of 80 °C under reflux. A predetermined quantity of polymer was dissolved in the solvent mixture gradually to avoid lump formation. After the complete dissolution of the added polymer, the remaining portion was introduced. A completely dissolved polymer solution was sonicated for 4 h to remove bubbles. Finally, a Pebax Rnew dope solution was poured into the glass Petri dish and covered with another properly leveled, bigger Petri dish with a slight opening at the bottom. The dope solution was left to evaporate at ambient temperature for at least 48 h and subsequently dried in an oven for at least 24 h at a temperature of 120 °C. After the complete removal of solvent, the membranes were gently peeled off from the Petri dish for performance studies.

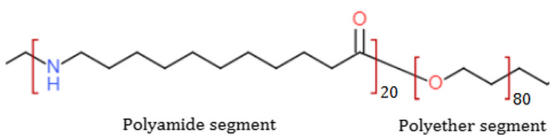

Fig. 1 Chemical structure of the Pebax® Rnew® 30R51 polymer.

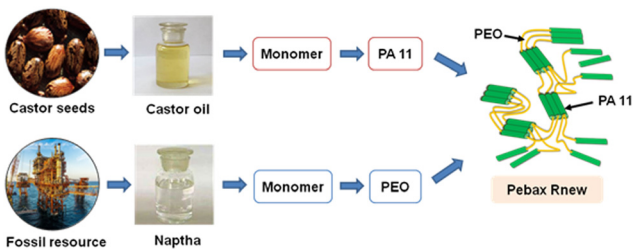

Fig. 2 Steps involved in synthesizing the Pebax® Rnew® 30R51 polymer.

2.3. Membrane characterization

FTIR spectra of the Pebax Rnew membranes were scanned between 4000 and 400 cm^{-1} using a PerkinElmer Spectrum Two™ spectrometer.

TGA of the synthesized membranes was performed under a N_2 atmosphere using a Discovery series (SDT 560) instrument at a heating rate of 10 °C min^{-1} to 800 °C.

SEM performed using a FEI Quanta 200 Field Emission scanning electron microscope was used to investigate the surface and cross-sectional morphologies of the synthesized membranes. Samples were prepared by dipping them in liquid nitrogen and coating them with conducting gold to avoid electron beam charging.

The intersegment distance between the polymer chains in membranes was confirmed on a Proto Advance X-ray diffractometer (XRD) connected to a Lynx eye high-speed strip detector. X-rays of 0.154 nm in wavelength were produced using a Cu Kα source. The angle (2θ) of diffraction was varied from 10° to 80° to identify the intersegmental chains.

2.4. Gas permeation studies

Fig. 3 shows a schematic of the membrane based gas permeation experimental system. The performance of the membranes was evaluated using an indigenously designed setup of SS 316 material. The experimental setup was flexible to perform both pure and mixed gas studies. The membrane test cell consists of two ports at the top for transporting feed and retentate gas and two at the bottom for transporting permeate and sweep gas. An inert gas such as helium or argon gas was used as the sweep gas. The top and bottom of the plates were connected by locking bolts. A perforated circular plate attached with fine SS mesh supported the membrane. Vacuum grease was used for the rubber gasket and "O" ring while fixing the membrane to avoid leaks. All the steams such as feed, retentate, permeate, and sweep gas lines were $\frac{1}{4}''$ tubes made of SS 316. Compression fitting nuts and ferrule were used for all streams to withstand higher pressures and avoid leakage. Feed, retentate, and sweep stream gas flows were regulated with $\frac{1}{4}''$ SS 316 needle valves.

The synthesized membranes were tested for pure CO_2, CH_4, H_2, O_2 and N_2 gases using the traditional constant pressure method. The permeability and selectivity were measured in the 2 to 10 bar pressure range and at ambient temperatures (25± 3 °C). Self-supported membranes were gently cut into circular form and placed over a polyester fabric support in the permeation test cell. A rubber gasket and "O" ring were placed on the membrane by applying vacuum grease. The top lid of the test cell was properly positioned to tighten the cell. The top and bottom lids were fixed appropriately using SS bolts. At least

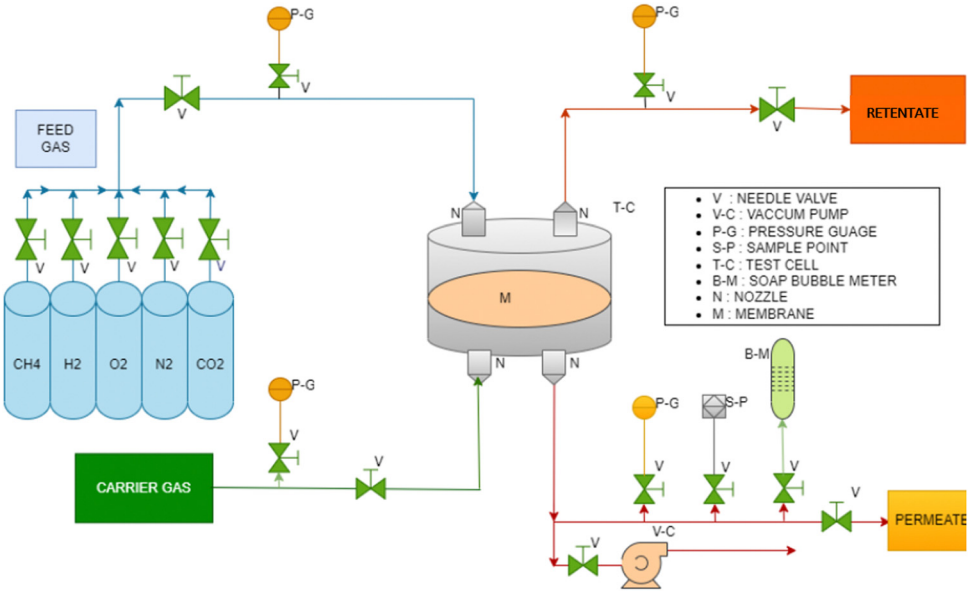

Fig. 3 Schematic of the gas permeation testing facility.

three samples were evaluated from each membrane type and the gas permeability was averaged. Sweep gas was not used in this case as transport gas as the permeate flow rate was measurable. Before every experiment, feed, retentate, and permeate streams were flushed with inert gas to avoid contamination. Feed gas was slowly passed into the top section of the membrane test cell using a needle valve. Continuous gas flow was maintained across the membrane in the test cell by partially opening the output valve. A soap bubble flow meter was fitted to the permeate line to measure the permeate flow. After attaining a steady state, the permeation data were collected at least five times over 30 min, and the calculated permeability was averaged. Synthesized membrane thicknesses were measured using SEM at different portions of the membrane cross-section, and the average value was used for calculating permeability.

The permeability coefficient (P) was calculated using eqn (1):

$$P = \frac{qt}{a \cdot (p_A - p_B)} \quad (1)$$

where q is the permeating gas flow rate (cm^3 s (STP)), t is the membrane thickness (cm), a is the membrane area (cm^2), and p_A and p_B are the feed and permeate side partial pressures (cm Hg), respectively. The membrane permeability was calculated in Barrer (1 Barrer = 10^{-10} (cm^3 (STP) cm cm^{-2} s^{-1} $cmHg^{-1}$)).

The selectivity (α) is the permeability ratio of fast and slow permeating gas.

$$\alpha = \frac{P_a}{P_b} \quad (2)$$

where P_a and P_b are the permeability of fast and slow permeating gas, respectively.

3. Results and discussion

3.1. Membrane characterization

3.1.1. SEM. SEM characterization was conducted to investigate the synthesized membrane surface and cross-section morphologies. Obtained membrane films were transparent and flexible. Fig. 4(a)–(d) represent the cross-section morphologies of 2 wt%, 4 wt%, 6 wt% and 8 wt% Pebax Rnew membranes, respectively. The exact quantity of polymer solution was added to the Petri dish for synthesizing the membranes. The cross-section morphologies show an increase in membrane thickness with increasing polymer concentration, as expected. In a lower polymer/solvent ratio mixture, less polymer is spread on a Petri dish and more solvent is evaporated, forming a thin membrane. In a higher polymer/solvent ratio, more polymer is spread on the Petri dish, forming a denser membrane matrix.[25] More Pebax Rnew polymer chains were distributed in the fixed Petri dish size at higher polymer concentrations, resulting in thick membranes and *vice versa*. All the membrane cross-sectional morphologies were dense and homogeneous without any porous structure.

Fig. 4(e)–(h) show the surface morphologies of 2 wt%, 4 wt%, 6 wt% and 8 wt% Pebax Rnew membranes, respectively. As observed in surface morphologies, the top surface of the membranes is homogeneous and uniform in nature; no defects or polymer agglomerations were detected. To avoid lump and agglomeration at higher polymer concentrations, precautions were taken to obtain defect-free and smooth membranes, such as casting the membrane when the polymer solution was around 30–35 °C, heating the Petri dishes at around 30 °C to avoid instantaneous evaporation of the solvent and covering them with larger Petri dishes with a very small opening.

3.1.2. FTIR spectroscopy. Fig. 5(a)–(d) show the FTIR spectra of the 2 wt%, 4 wt%, 6 wt% and 8 wt% Pebax Rnew membranes, respectively. All four membranes show similar spectra patterns,

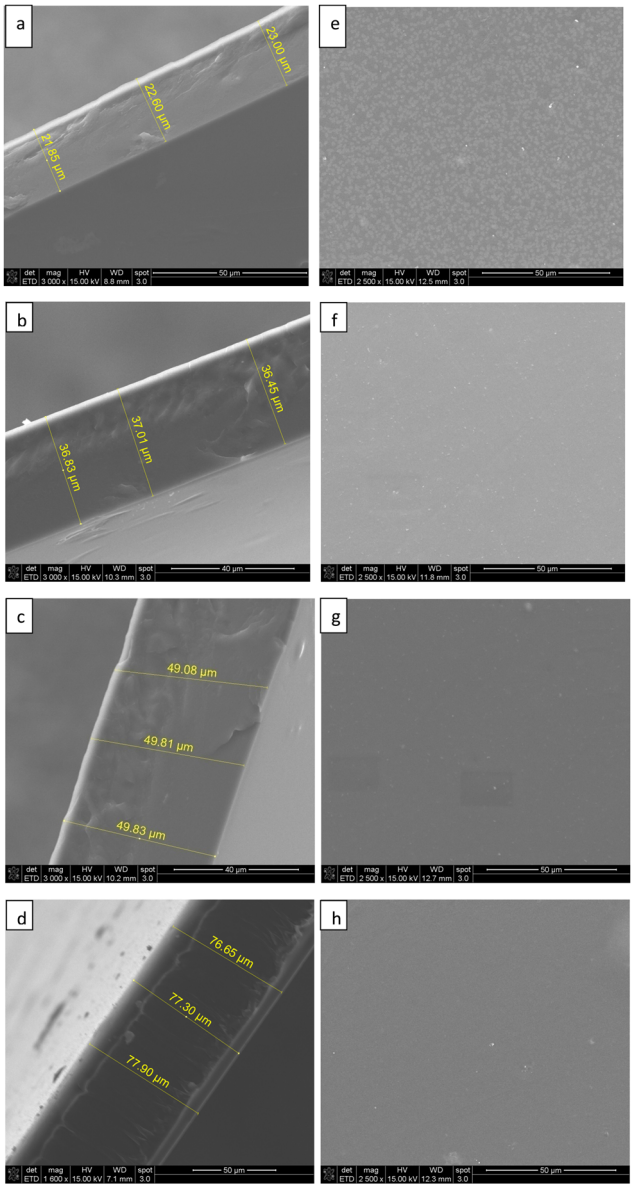

Fig. 4 Cross-section morphologies of (a) 2 wt%, (b) 4 wt%, (c) 6 wt% and (d) 8 wt% Pebax Rnew membranes, and surface morphologies of (e) 2 wt%, (f) 4 wt%, (g) 6 wt% and (h) 8 wt% Pebax Rnew membranes.

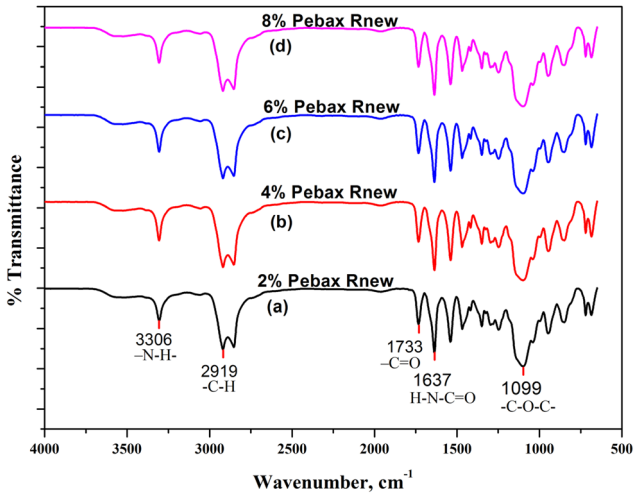

Fig. 5 FTIR spectra of the (a) 2 wt%, (b) 4 wt%, (c) 6 wt% and (d) 8 wt% Pebax Rnew membranes.

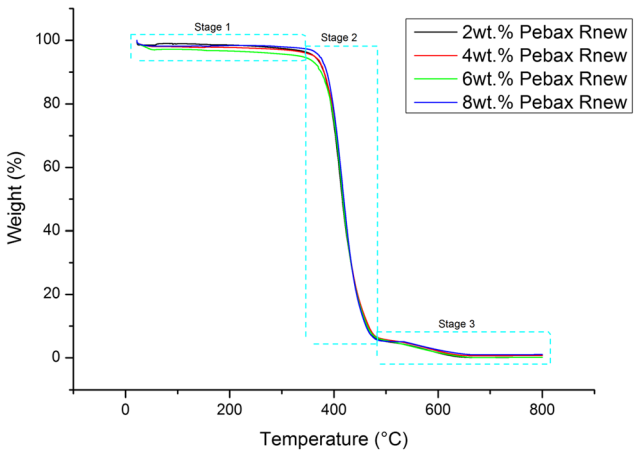

Fig. 6 TGA curves of the 2 wt%, 4 wt%, 6 wt% and 8 wt% Pebax Rnew membranes.

featuring polyamide and polyether domains. The peak at 1637 cm^{-1} represents the stretching vibrations of the H–N–C═O functional group, the peak at 1733 cm^{-1} is associated with the –C═O group in saturated esters, and the peak at 3306 cm^{-1} represents the –N–H– groups.[8] Regarding the polyether soft segment bands, the peak at 2919 cm^{-1} represents the aliphatic C–H functional group stretching and bending vibrations. The pattern obtained at 1099 cm^{-1} corresponds to the stretching vibration of the C–O–C ether functional group. The peaks align with the reported literature.[8,17,26]

3.1.3. TGA. TGA characterization of the synthesized membranes was conducted under a N_2 atmosphere at a heating rate of 10 °C min^{-1} in a 20–800 °C temperature range. Fig. 6 illustrates the weight variation of Pebax Rnew membranes tested in this study during the heating process. The TGA results of 2 wt%, 4 wt%, 6 wt% and 8 wt% Pebax Rnew membranes follow the same trend in weight loss with increasing temperature. No weight loss was observed for all the membranes tested ≤100 °C, representing complete moisture and solvent removal from the membrane matrix. From Fig. 6, three stages of membrane degradation were observed with temperature. Stage 1 refers to the thermal rearrangement of the polymer with increasing temperature. The Pebax Rnew membranes exhibited excellent thermal stability up to 340 °C. In stage 2, with increasing the temperature beyond 340 °C, the sample starts decomposed drastically; an enormous weight decrease was observed, and maximum degradation was observed at 475 °C. This represents the oxidation mechanism, wherein the combustion of residues of the thermal degradation and aromatic compounds occurred.[22] There was more weight loss in the 6 wt% Pebax Rnew membranes compared to the other membranes, in both stages 1 and 2. Reduced membrane crystallinity and higher polymer chain mobility might have decreased the

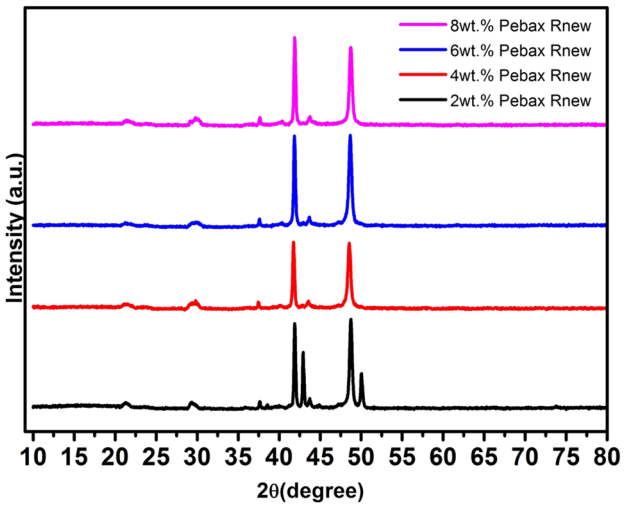

Fig. 7 XRD patterns of the 2 wt%, 4 wt%, 6 wt% and 8 wt% Pebax Rnew membranes.

intra and inter polymeric chain interactions, which led to a reduction in the thermal stability.[23] Lower polymer concentration might have facilitated easy interaction between the polymer chains, which helped to promote a more favorable polymer chain orientation to enhance the polymer–polymer interactions.[19] Surprisingly, for the 8 wt% Pebax Rnew membrane, a slight increase in thermal stability occurred due to polymer chain entanglement. In stage 3, the degradation from 475 °C corresponded to the carbonization of the degraded polymer matrix. A significant change in the final degradation temperature was not observed by varying the concentration of Pebax Rnew in the casting solution.

3.1.4. XRD. Fig. 7 illustrates the XRD patterns of the Pebax Rnew polymer membranes. All the synthesized membranes showed similar diffraction peaks. Pebax Rnew is a semicrystalline polymer with crystalline and amorphous phases of both PEO and PA. The diffraction peaks at 21°, 29°, and 42° of 2θ represent the amorphous nature, and the peaks at 41° and 48° of 2θ correspond to the crystalline nature of the polymer. The 2 wt% Pebax Rnew membrane exhibited more crystalline character compared to the other membranes. In agreement with the literature, increasing the polymer concentration decreased the crystallinity.[22] It is evident from the XRD patterns of 4, 6 and 8 wt% Pebax Rnew that the ordering of the polymer chains along certain crystallographic planes disappeared, resulting in a complete loss in intensity from that direction. Increasing the polymer solution concentration, the patterns slightly shifted to the left, revealing an increase in intersegmental spacing. With increasing polymer concentration, the structural relaxation time increased, which resulted in more chain flexibility. This molecular mobility and polymer chain arrangement increased the intersegmental spacing. This marginal increase in intersegmental spacing might have enhanced the amorphous nature of the polymer and membrane permeability.

3.2. Gas permeation studies

3.2.1. Effect of polymer solution concentration. The Pebax block copolymer is a combination of glassy polyamide segments and rubbery polyether segments. Different grades of Pebax have emerged as potentially attractive membrane materials for gas- and liquid-based separation applications. Table 1 shows that the Pebax Rnew polymer consists of a higher percentage (80%) of rubbery segments compared to other grades of Pebax such as 1657, 3533, and 4533. Due to the higher amount of flexible domains in the Pebax Rnew polymer, primary gas permeation occurs *via* the rubbery segments. Because of their highly crystalline nature and their lower proportion in the Pebax Rnew polymer, the sorption contribution of the glassy domains is insignificant.[9] The polyamide phase in Pebax Rnew, PA11, represents 10 methyl functional groups and plays a significant role in the permeation of gases. Generally, the higher the chain length, the poorer the chain packing efficiency, which leads to more free volume and, therefore, a higher gas diffusion.[27]

Table 2 shows the effect of the Pebax Rnew polymer solution concentration on the gas permeation characteristics at a constant feed gas pressure of 5 bar. The gas permeability order was observed to be $CO_2 > H_2 > CH_4 > O_2 > N_2$. CO_2 gas showed higher solubility in the Pebax Rnew polymer and is comparatively inert to the other gases. The polyether segments in the Pebax Rnew are strongly associated with CO_2 because of dipole-quadrupole interactions between the polyether matrix and CO_2 molecule.[8,28] Due to the higher amount of soft segments in the Pebax Rnew polymer, the CO_2 solubility and permeability values are higher. Additionally, the kinetic diameter of CO_2 is less than those of CH_4, O_2 and N_2, leading to it exhibiting higher diffusivity than the other gases. In the case of H_2, diffusivity would be higher than CO_2 due to its smaller kinetic diameter (2.89 Å) than that of CO_2 (3.3 Å). However, the selectivity of gas molecules depends on their condensability and polymer–gas interactions. Typically for rubbery polymers, CO_2 has greater solubility than H_2.[29–31] The higher polyether content in Pebax typically resulted in higher gas solubility, and, in addition, quadrupolar interactions between the CO_2 molecules and the ether groups enhanced the solubility.[32] Hence, despite its smaller kinematic diameter (2.89 Å), H_2 exhibited less permeability in the polymer matrix. CH_4, H_2, N_2 and O_2

Table 2 Effect of the Pebax Rnew polymer solution concentration on the gas permeation

		Gas permeability (Barrer)				
Membrane	Average thickness (μm)	CO_2	CH_4	O_2	N_2	H_2
2% Pebax Rnew	22	113 ± 3	5.3 ± 0.1	4.1 ± 0.1	1.8 ± 0.1	9.5 ± 0.2
4% Pebax Rnew	36	112 ± 4	5.3 ± 0.2	4.8 ± 0.1	1.7 ± 0.1	9.3 ± 0.2
6% Pebax Rnew	50	205 ± 6	9.6 ± 0.2	8.1 ± 0.2	2.9 ± 0.1	18.6 ± 0.9
8% Pebax Rnew	76	136 ± 5	8.0 ± 0.2	4.9 ± 0.1	2.2 ± 0.1	12.6 ± 0.8

transport was due to the polyamide phase free volume in the polymer.

From Table 2, it was found that increasing the polymer concentration from 2 wt% to 4 wt% had no impact on the gas permeability. At 6 wt% of Pebax Rnew polymer concentration, around 85%, 80%, 100%, 60% and 90% increases in gas permeation were observed for CO_2, CH_4, O_2, N_2 and H_2 gases, respectively. The increase in permeability was due to the polymer matrix arrangement and change in intersegmental spacing with polymer solution concentration, as shown in the XRD data. Fig. 8 shows the mechanism of gas permeation through the membrane upon varying the polymer concentration. For 2 wt% and 4 wt% polymer concentrations, the structural relaxation time was low due to fast solvent evaporation. Polymer chains are not very flexible for orientation and result in less free volume. At a critical concentration of 6 wt%, the polymer chains have sufficient time for chain alignment and ensure more free volume. The increased free volume enhances the gas permeation through the polymer matrix. Additionally, the higher amount of soft segments in 6 wt% compared with 2 wt% and 4 wt% led to higher permeation of gases. Thus, higher gas permeability was observed for all the gases. However, at a higher polymer concentration of 8 wt%, gas permeability was decreased for all the gases. This might be due to the higher packing density of the polyamide and polyether segments on the membrane surface. A higher packing density would have compacted the polymer matrix and decreased the fractional free volume, as shown in Fig. 8. Fig. 9 illustrates the effect of polymer solution concentration on the selectivity of CO_2/N_2, CO_2/H_2, CO_2/CH_4, H_2/N_2, CH_4/N_2 and O_2/N_2. Though the permeability of gases was enhanced considerably, significant improvement in gas selectivity was not observed, except for CO_2/N_2 gas system. Hence, the 6 wt% Pebax Rnew polymer was considered to be the optimal polymer solution concentration for the best gas separation performance.

3.2.2. Effect of feed pressure. The effect of pressure on 6 wt% Pebax Rnew membrane permeability and selectivity was investigated by varying the feed pressure from 2 to 10 bar in intervals of 2 bar. With increasing pressure, the permeability of all the gases increased, as shown in Table 3, due to increased driving force and solubility. CO_2 gas permeability improved significantly by around 120% compared to H_2, N_2, O_2 and CH_4. This is owing to the quadrupole dipole moment force of the ether groups in the membranes towards CO_2 and the self-compressible properties of CO_2.[33] A higher pressure tends to enhance the solubility and driving force of CO_2, leading to a higher permeability. In the case of H_2, CH_4, N_2 and O_2 gases, permeability increased marginally from 16.1 to 25.6 Barrer, 7.6 to 13.9 Barrer, 2.4 to 3.8 Barrer and 6.5 to 11.5 Barrer, respectively, upon increasing the pressure. A decrease in free volume fraction with pressure might have restricted the gas diffusivity through the membrane matrix.

The effect of applied feed pressure on membrane selectivity is shown in Fig. 10. CO_2/N_2, CO_2/CH_4 and CO_2/H_2 gas selectivity enhanced from 65 to 91, 20 to 25 and 9 to 13, respectively, with increasing pressure. The increase in CO_2 gas selectivity to N_2, CH_4 and H_2 gases was anticipated due to the plasticization of polymer chains by CO_2 molecules with increasing pressure. Another possibility is that the flexible polyether segments' weak size sieving capability results in high CO_2 selectivity. Increasing

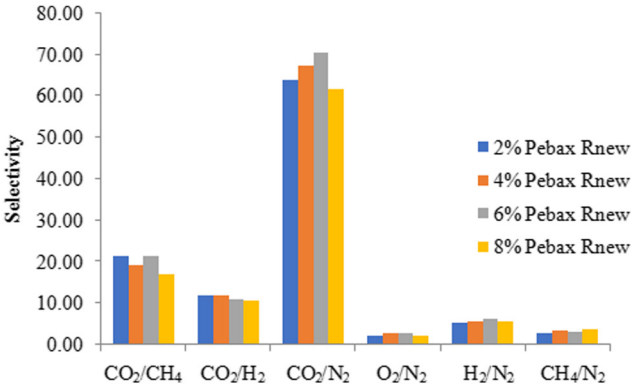

Fig. 9 Effect of polymer solution concentration on the gas selectivity.

Table 3 Effect of feed pressure on the permeability using 6 wt% Pebax Rnew membrane

	Gas permeability (Barrer)				
Pressure (bar)	CO_2	CH_4	N_2	H_2	O_2
2	156.6	7.6	2.4	16.1	6.5
4	186.5	8.2	2.75	17.5	7.2
6	240.1	10.6	3.12	20.1	8.9
8	280.6	12.1	3.4	23.5	9.2
10	346.2	13.9	3.8	25.6	11.5

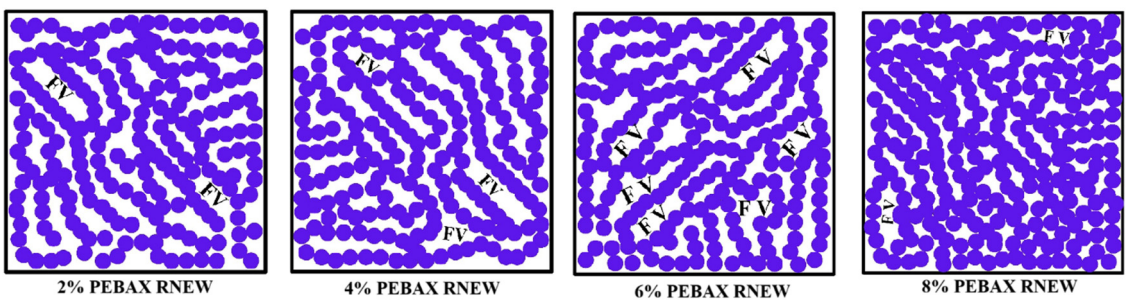

Fig. 8 Mechanism of gas permeation through the membranes upon varying the polymer concentration.

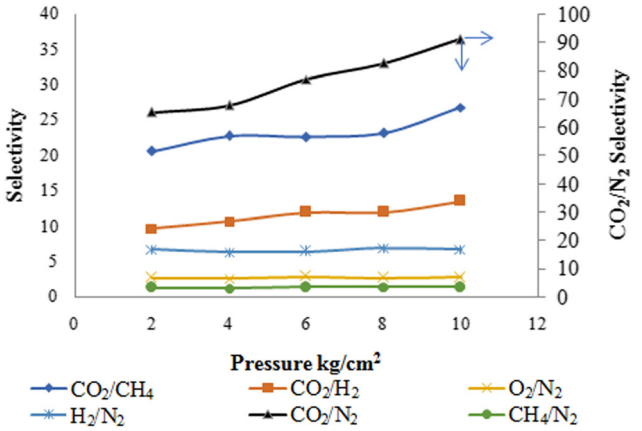

Fig. 10 Effect of feed pressure on gas selectivity using the 6 wt% Pebax Rnew membrane.

pressure had a marginal change effect on CH_4/N_2, H_2/N_2 and O_2/N_2 gas selectivities.

3.2.3. Comparison with literature. To the best of our knowledge, Pebax Rnew membranes gas permeation was evaluated for CO_2, N_2 and CH_4 and was not previously reported for O_2 and H_2 gases within the open literature. Different grades of Pebax have been evaluated by varying polymer concentrations for gas separation performance; however, the literature on biobased Pebax Rnew is limited. Table 4 compares the performance of different grades of Pebax membranes evaluated in the same concentration range (2–3 wt%). Compared to other grades, Pebax Rnew membranes exhibit superior separation performance due to a higher content of flexible PEO. Martínez-Izquierdo *et al.* reported a Pebax Rnew membrane selectivity of around 51 and 10 for CO_2/N_2 and CO_2/CH_4, respectively.[8,17] In this study, the 2 wt% Pebax Rnew membrane exhibited a higher selectivity of around 65 and 20 for CO_2/N_2 and CO_2/CH_4, respectively. By varying the polymer concentration, a higher selectivity of around 70 and 26 for CO_2/N_2 and CO_2/CH_4, respectively, was achieved. There is great scope to work on Pebax Rnew membrane synthesis parameters, such as the effect of solvents and mixtures, casting parameters and post-treatment of membranes. The performance of membranes with gas mixtures and membrane limitations, such as plasticization and aging effects, could be further evaluated.

4. Conclusions

Biobased Pebax® Rnew® 30R51 membranes were successfully prepared in a 1:1 (v/v) solvent mixture of 1-butanol and 1-propanol. Dense membranes were synthesized by varying the polymer concentration from 2 wt% to 8 wt%. The performances of the synthesized membranes were evaluated for pure CO_2, CH_4, H_2, N_2 and O_2 gases. SEM morphologies show an increase in membrane thickness with increasing polymer concentration due to the change in the polymer/solvent ratio of the Pebax Rnew solution. The FTIR spectra showed a similar pattern for all the synthesized membranes. Both polyamide and polyether segment bands were observed in the spectra. The TGA results of the Pebax Rnew membranes follow the same trend in weight loss with increasing temperature, with these membranes exhibiting excellent thermal stability up to 340 °C. The XRD patterns reveal an increase in intersegmental spacing with polymer solution concentration.

The order of gas permeability was observed to be: $CO_2 > H_2 > CH_4 > O_2 > N_2$. Due to the higher content of the soft rubbery segments in the Pebax Rnew polymer, CO_2 solubility and transport across the membrane were easier. The permeability of the other gases was relatively low due to them being inert toward the polymer matrix. The membranes prepared from 6 wt% Pebax Rnew solution were identified as highly permeable and selective. The highest selectivities of 91, 13 and 26 were observed for CO_2/N_2, CO_2/H_2 and CO_2/CH_4, respectively, with increasing pressure. The developed biobased Pebax Rnew membrane holds potential for CO_2 separation from power plants, sweetening of natural gas and water–gas shift reaction applications. Unlike other Pebax grades, research on the Pebax Rnew membrane is limited. There is great scope to work on other parameters, such as the effect of solvents and mixtures, casting parameters and post-treatment of membranes. Separation properties could be further improved by physical and chemical modification of the Pebax Rnew membrane. The performance of membranes with gas mixtures and impurities could be studied. In addition, membrane limitations, such as plasticization and aging effects, could be assessed deeply. The Pebax Rnew thin film composite membrane can be easily scaled into spiral wound modules for high-pressure separation processes such as natural-gas sweetening.

Table 4 Comparison of Pebax Rnew membrane performance with the literature data

	Permeability (Barrer)			Selectivity		
Polymer conc.	CO_2	N_2	CH_4	CO_2/N_2	CO_2/CH_4	Ref.
3 wt% Pebax 1657	92 ± 4	2.2 ± 0.2	—	39 ± 6		22
2.5 wt% Pebax 1657	123.4 ± 3.7	—	5.8 ± 0.17	—	21.2 ± 1.1	34
3 wt% Pebax 1074	170	4.1	—	41	—	35
2.5 wt% Pebax 1074	63	—	2.8	—	22	36
3 wt% Pebax 2533	238 ± 8	12.4 ± 0.3		19 ± 1		8
3 wt% Pebax 3533	205 ± 13	13.0 ± 9.5		22 ± 1		8
3 wt% Pebax 4533	97 ± 10	10.0 ± 5.7		18 ± 3		8
3 wt% Pebax Rnew	167 ± 7	4.1 ± 0.1	—	41 ± 3	—	8
2 wt% Pebax Rnew	497 ± 71[a]	21 ± 4[a]	49 ± 5[a]	27 ± 3	9 ± 2	17
2 wt% Pebax Rnew	113 ± 3	5.3 ± 0.1	1.8 ± 0.1	62 ± 2	20 ± 2	This work

[a] GPU = gas permeation unit.

Conflicts of interest

There are no conflicts to declare.

References

1 M. Chawla, H. Saulat, M. Masood Khan, M. Mahmood Khan, S. Rafiq, L. Cheng, T. Iqbal, M. I. Rasheed, M. Z. Farooq, M. Saeed, N. M. Ahmad, M. B. Khan Niazi, S. Saqib, F. Jamil, A. Mukhtar and N. Muhammad, *Chem. Eng. Technol.*, 2020, **43**, 184–199.
2 C. E. Powell and G. G. Qiao, *J. Membr. Sci.*, 2006, **279**, 1–49.
3 Y. Zhang, J. Sunarso, S. Liu and R. Wang, *Int. J. Greenhouse Gas Control*, 2013, **12**, 84–107.
4 M. S. Shin, K.-H. Jung, J.-H. Kwag and Y.-W. Jeon, *Process Saf. Environ. Prot.*, 2019, **129**, 348–358.
5 N. Sazali, M. A. Mohamed and W. N. W. Salleh, *Int. J. Adv. Manuf. Technol.*, 2020, **107**, 1859–1881.
6 N. W. Ockwig and T. M. Nenoff, *Chem. Rev.*, 2007, **107**, 4078–4110.
7 R. S. Murali, T. Sankarshana and S. Sridhar, *Sep. Purif. Rev.*, 2013, **42**, 130–186.
8 L. Martínez-Izquierdo, A. Perea-Cachero, M. Malankowska, C. Téllez and J. Coronas, *J. Environ. Chem. Eng.*, 2022, **10**, 108324.
9 R. Surya Murali, S. Sridhar, T. Sankarshana and Y. V. L. Ravikumar, *Ind. Eng. Chem. Res.*, 2010, **49**, 6530–6538.
10 P. Sharma, Y.-J. Kim, M.-Z. Kim, S. F. Alam and C. H. Cho, *Nanoscale Adv.*, 2019, **1**, 2633–2644.
11 V. I. Bondar, B. D. Freeman and I. Pinnau, *J. Polym. Sci., Part B: Polym. Phys.*, 1999, **37**, 2463–2475.
12 P. Bernardo and G. Clarizia, *Polymers*, 2020, **12**, 253.
13 H. Hassanzadeh, R. Abedini and M. Ghorbani, *Ind. Eng. Chem. Res.*, 2022, **61**, 13669–13682.
14 N. Azizi, T. Mohammadi and R. Mosayebi Behbahani, *Chem. Eng. Res. Des.*, 2017, **117**, 177–189.
15 L. Martínez-Izquierdo, M. Malankowska, C. Téllez and J. Coronas, *J. Environ. Chem. Eng.*, 2021, **9**, 105624.
16 K. Friess, V. Hynek, M. Šípek, W. M. Kujawski, O. Vopička, M. Zgažar and M. W. Kujawski, *Sep. Purif. Technol.*, 2011, **80**, 418–427.
17 L. Martínez-Izquierdo, C. Téllez and J. Coronas, *J. Mater. Chem. A*, 2022, **10**, 18822–18833.
18 R. M. Cywar, N. A. Rorrer, C. B. Hoyt, G. T. Beckham and E. Y. X. Chen, *Nat. Rev. Mater.*, 2022, **7**, 83–103.
19 T. M. Joseph, A. B. Unni, K. S. Joshy, D. Kar Mahapatra, J. Haponiuk and S. Thomas, *C*, 2023, **9**, 30.
20 P. M. Aparna Shukla, *Advances in Sustainable Polymers: Processing and Applications*, ed. V. Katiyar, R. Gupta and T. Ghosh, Springer Nature Singapore Pte Ltd, 2019, pp. 3–19.
21 M. Schär, L. Zweifel, D. Arslan, S. Grieder, C. Maurer and C. Brauner, *Polymers*, 2022, **14**, 5092.
22 L. Martínez-Izquierdo, M. Malankowska, J. Sánchez-Laínez, C. Téllez and J. Coronas, *R. Soc. Open Sci.*, 2019, DOI: **10.1098/rsos.190866**.
23 M. R. Hasan, H. Zhao, N. Steunou, C. Serre, M. Malankowska, C. Téllez and J. Coronas, *Int. J. Greenhouse Gas Control*, 2022, **121**, 103791.
24 Arkema, High performance bio-based materials for sports, **https://hpp.arkema.com/files/live/sites/hpp_extrememateriales/files/downloads/market-presentations/arkema-mp-sports-market-presentation.pdf**.
25 S. S. Karim, S. Farrukh, A. Hussain, M. Younas and T. Noor, *Polym. Polym. Compos.*, 2022, **30**, DOI: **10.1177/09673911221090053**.
26 H. Sanaeepur, S. Mashhadikhan, G. Mardassi, A. Ebadi Amooghin, B. Van der Bruggen and A. Moghadassi, *Korean J. Chem. Eng.*, 2019, **36**, 1339–1349.
27 S. Wang, Y. Liu, S. Huang, H. Wu, Y. Li, Z. Tian and Z. Jiang, *J. Membr. Sci.*, 2014, **460**, 62–70.
28 D. Zhao, J. Ren, H. Li, X. Li and M. Deng, *J. Membr. Sci.*, 2014, **467**, 41–47.
29 R. W. Baker, E. L. Cussler, W. Eykamp, W. J. Koros, R. L. Riley and H. Strathmann, *Membrane separation systems—A research and development needs assessment*, 1990.
30 B. E. Poling, J. M. Prausnitz and J. P. O'Connell, *The Properties of Gases and Liquids*, McGraw-Hill, New York, 4th edn, 1987.
31 E. Esposito, R. Bruno, M. Monteleone, A. Fuoco, J. Ferrando Soria, E. Pardo, D. Armentano and J. C. Jansen, *Appl. Sci.*, 2020, **10**, 1310.
32 S. L. Liu, L. Shao, M. L. Chua, C. H. Lau, H. Wang and S. Quan, *Prog. Polym. Sci.*, 2013, **38**, 1089–1120.
33 X. Guan, Y. Wu, Y. Zheng and B. Zhang, *Sci. Prog.*, 2023, **106**, 1–19.
34 Z. Farashi, S. Azizi, M. Rezaei-Dasht Arzhandi, Z. Noroozi and N. Azizi, *J. Nat. Gas Sci. Eng.*, 2019, **72**, 103019.
35 Y. Wang, H. Li, G. Dong, C. Scholes and V. Chen, *Ind. Eng. Chem. Res.*, 2015, **54**, 7273–7283.
36 S. Azizi, N. Azizi and R. Homayoon, *Silicon*, 2019, **11**, 2045–2057.